Intrinsic Si Quantum Efficiency, Sensitivity, and Other Parameters Temperature Dependence for BSI Image Sensors

Sergey Velichko[1], Bob Gravelle[1], Daniel Tekleab[2], Michael Guidash[2], Scott Johnson[1], Minseok Oh[2], Hung Chih Chang[2]
[1]ON Semiconductor, Meridian, ID, USA, [2]ON Semiconductor, Santa Clara, CA, USA
sergey.velichko@onsemi.com

***Abstract*—We discussed temperature dependencies of quantum efficiency (QE), sensitivity, color effects, and other pixel parameters for backside illuminated image sensors. According to the modeling and measurements, QE defines sensitivity temperature dependence and also impacts differently for visual color and near-IR bands. Comparing +120ºC junction vs. room temperature, in visual range we measured few relative percent increase while in 940 nm band range we measured 1.46x increase in sensitivity. Measured pixel source follower and transaction factor gains vs. temperature contributed to pixel output signal slope. Measured impact of sensitivity for visual bands, such as blue, green, and red colors, reflected some impact to captured image color accuracy that created slight image color tint at high temperature. The tint is, however, hard to detect visually and may be removed by auto white balancing and temperature adjusted color correction matrixes.**

Keywords—image sensor; quantum efficiency; CMOS; sensitivity; temperature dependence

I. Introduction

Image sensors with unsurpassed high dynamic range (HDR) and light flicker mitigation performance [1, 2] are powering the latest advancements in autonomous and assisting driving. These sensors employ CMOS back side illumination (BSI) technology to consistently outperform sensors of the previous generations.

These sensors operate in the automotive temperature range from -40ºC to +125ºC while providing clear, colorful, and crisp images suitable for small object recognition with high probability. This work studied the impact of this wide temperature range on HDR BSI sensor's characteristics. The effects investigated included quantum efficiency (QE), sensitivity, source follower (SF) gain, pixel transaction factor (PTF) gain, color ratios, and color image quality.

II. Modeling

The Si absorption coefficient behavior across different light wavelengths has been well studied [3]. Its dependence on temperature conforms to a power law [4].

We used a 2D pixel model with no optical stack similar to Fig. 1 to perform electro-optical simulations of the QE temperature dependency and consequent sensor sensitivity. The simulations used a Transfer Matrix Method (TMM) optical solver along with n&k values obtained from [4].

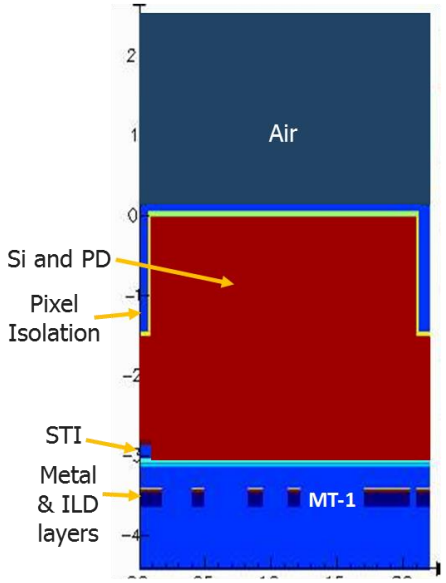

Fig. 1. Pixel simulation model.

In addition, models for Si bandgap narrowing and SRH effects were included in the pixel simulations. The pixel model utilized no µlens, no CFA, and no Si anti-reflective (ARC) layers, thus the pure Si effect was studied. Simulations demonstrated that QE depends on temperature due to strong effect of temperature on the Si absorption coefficient as shown in Fig. 2.

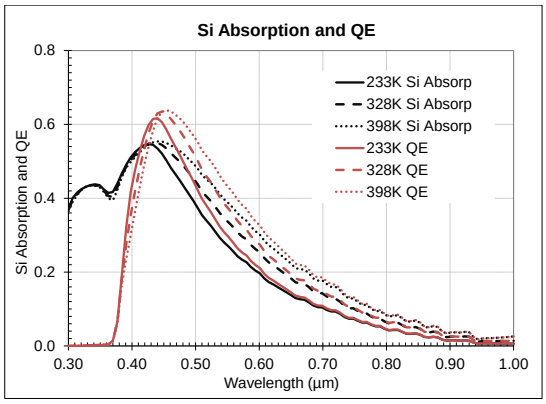

Fig. 2. Simulated Si absorption and quantum efficiency across different temperatures for pixel without µlens, CFA, and Si ARC.

We defined image sensor sensitivity and its temperature dependence as integral product:

$$S(T) = \int_{350nm}^{1150nm} I_s(\lambda) \bullet T_{lens}(\lambda) \bullet T_{IRCF}(\lambda) \bullet QE(T,\lambda) \bullet A_p d\lambda \ , \quad (1)$$

where $I_s(\lambda)$ is incoming light power, T_{lens} is lens transmission, T_{IRCF} is camera filter transmission, $QE(T, \lambda)$ is pixel quantum efficiency, and A_p is pixel area.

Assuming that incoming light spectra, area of the pixel, and lens and filter transmissions do not change with temperature we concluded that only QE defines image sensor sensitivity temperature dependence.

III. Source Follower and Pixel Transaction Factor Gain vs. Temperature

To understand the temperature impact from the shifting pixel parameters such as SF and PTF gains we performed measurements on five sensor sites across a wafer. Temperature dependency of the SF gain was studied before in consumer range from -20ºC to +80ºC [6], we extended the range to cover entire automotive range from -40ºC to +200ºC.

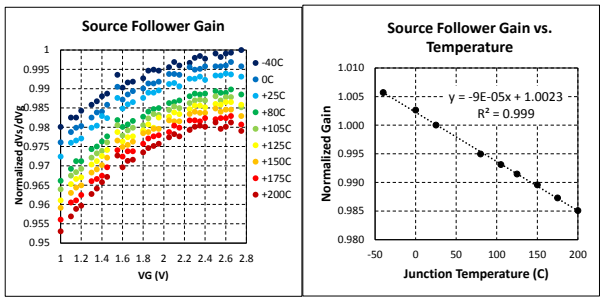

Fig. 3. Normalized measurement results of the SF gain across automotive temperature range.

In Fig. 1 we presented normalized averaged results of these SF gain measurements. When temperature increases, mobility of majority carrier decreases due to the increase of phonon scattering. As a result, transconductance and SF gain decreases accordingly.

Presented SF gain measurements showed reverse trend vs. temperature, earlier studies on pixel conversion and amplifier gains showed same trend [6], then measured normalized PTF gains (DN/e-) for both low (LCG) and high (HCG) conversion gains showed the similar temperature trends as depicted in Fig. 4.

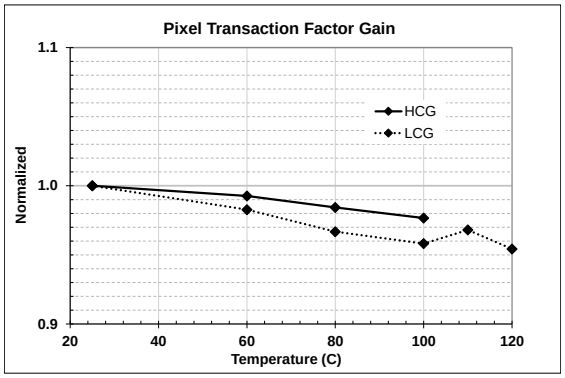

Fig. 4. Measurement results of the pixel transaction factor gains across automotive temperature range.

Measured LCG and HCG PTF gains reflected combined effect from the temperature dependencies of the pixel SF, floating diffusion, in-pixel capacitor node, and pixel amplifier. Measured pixel SF and PTF gains vs. temperature contributed to pixel output signal slope and were factored into further analysis.

IV. Quantum Efficiency, Sensitivity, and Color Ratios vs. Temperature

To extract sensitivity numbers for visual and near-infrared (NIR) ranges from the measured QE data we used relative light power spectral distributions and filter transmissions for both IR-cut (IRCF) and narrow band color and near-IR filters (NBFs) as shown in Fig. 3.

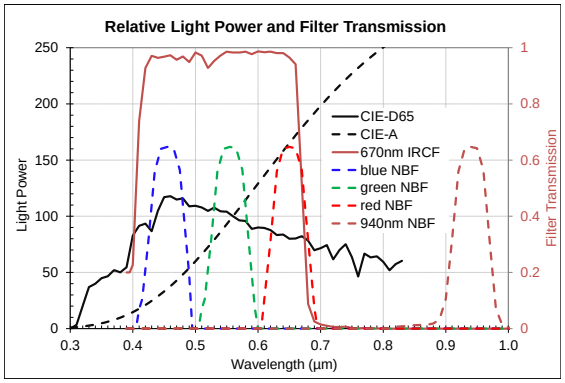

Fig. 4. Relative light power spectral distributions and filter transmissions used for sensitivity extraction in visual and NIR ranges.

Both CIE-D65 and CIE-A data sets are referenced in CIE publications [5].

We measured QE from 390nm to 1100nm for three samples each of a 3µm BSI sensor [2] and a 2.2µm BSI sensor using a monochromator setup with a 5nm grating and a NIST calibrated photodiode for reference. Averaged measured QE as well as extracted sensitivity data across different temperatures was normalized to room temperature 300ºK data set.

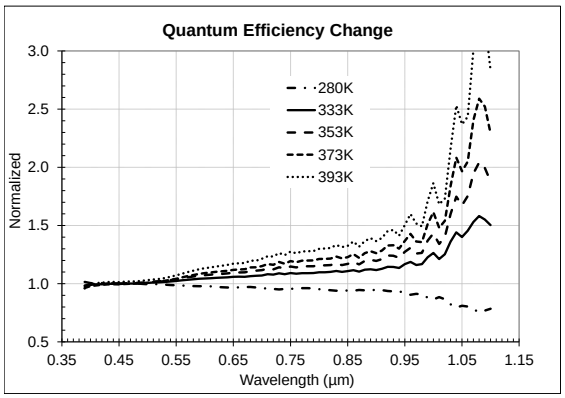

Fig. 5. Measured normalized quantum efficiency change across different temperatures for 3µm BSI sensor 1.

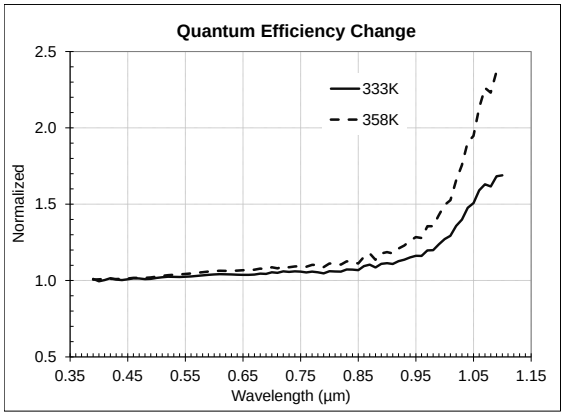

Fig. 6. Measured normalized quantum efficiency change across different temperatures for 2.2µm BSI sensor 2.

In Fig. 5 we presented the QE change for the 3µm sensor and in Fig. 6 for the 2.2µm sensor correspondingly. Analysis of the data showed close matching of the observed QE behavior for both sensors with some differences that may be, probably, attributed to optical stack and Si thickness variances. Temperature QE change across the wavelength follows a power law with biggest change in near-IR and relatively small change in visual range.

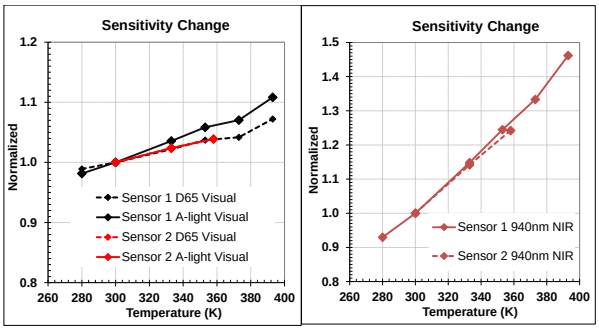

a) b)

Fig. 7. Normalized sensitivity change in visual (a) and NIR (b) ranges for both sensors.

Applying eq. 1 to D65, A-light, and measured QE data we extracted both wide band 670 nm IRCF visual and 940nm NBF NIR normalized sensitivities and presented them in Fig. 7. Sensitivity differences in the visual range were only a few relative percent comparing high temperature vs. room temperature. There was slight difference in D65 and A-light sensitivity behavior one sensor vs. another, attributable, probably, to the optical stack variances. In the NIR range, we observed relatively similar behavior for both sensors and a significant increase up to 1.46x for 940nm band at +120ºC.

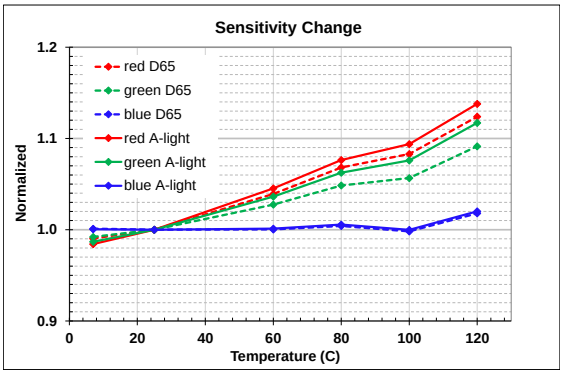

Fig. 8. Normalized color sensitivity change vs. temperature.

Applying eq. 1 with different filters (blue, green, and red bands) to measured QE data set, we studied color sensitivity changes. Fig. 8 presents normalized color sensitivities for D65 and A-light spectra correspondingly. Based on QE change vs. temperature, blue color band sensitivity change was minimal, red color sensitivity change was largest, and green color band sensitivity change was in between. All color sensitivity changes followed a linear behavior vs. temperature with the exclusion of +100ºC temperature point. We need more studies to understand the impact of the water boiling temperature point onto QE and sensitivity. Some small difference of the change in relation to the incoming light spectra D65 vs. A-light was observed, attributable to

better absorption of longer wavelength photons vs. temperature, that also impacted red/green (R/G) and blue/green (B/G) color ratios.

In Fig. 10 we presented R/G and B/G color ratios impact vs. temperature for both D65 and A-light sources.

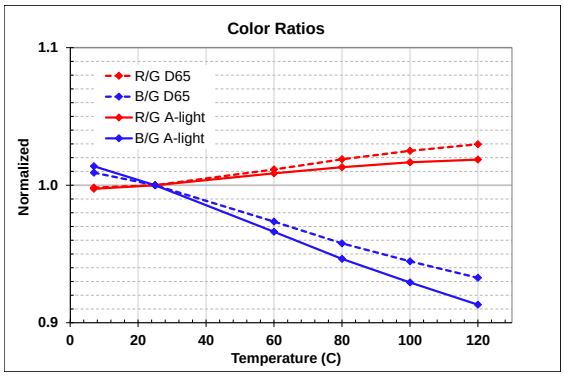

Fig. 9. D65 and A-light R/G and B/G color ratio change vs. temperature.

Wider spread of the R/G and B/G color ratios at high temperatures may impact sensor color image accuracy. More spread would result in some color tinting. To validate the color accuracy impact we captured Macbeth chart images at room and high temperature equivalent to +120ºC junction.

In Fig. 10 we presented Macbeth chart room temperature image capture at left and high temperature image capture at right.

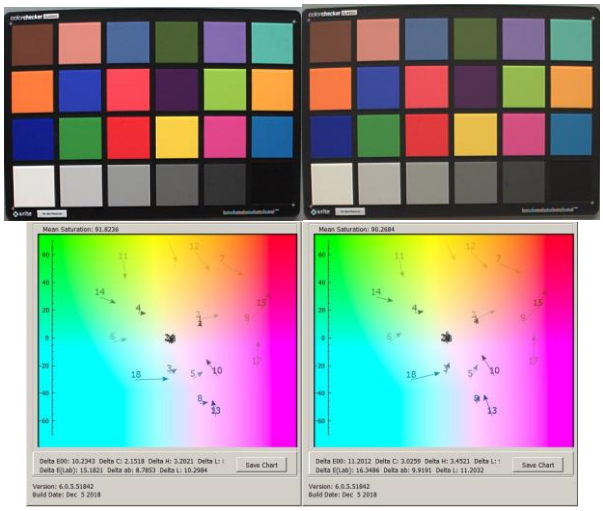

Fig. 11. Macbeth chart images and their corresponding color accuracy at room (left) and 120ºC junction (right) temperatures.

Measured above change of the blue, green, and red color band sensitivity reflected some impact to captured image color accuracy, ex. Macbeth chart dE=10.2 at room temperature vs. dE=11.2 at 120ºC temperature. High temperature impact on Macbeth chart color accuracy was not large and created slight image color tint that is hard to detect visually on the captured image.

V. Conclusion

We discussed temperature dependencies of QE, sensitivity, color effects, and other pixel parameters for backside illuminated image sensors. According to the modeling and measurements, QE defines sensitivity temperature dependence and also impacts differently for visual color and near-IR bands. Comparing +120ºC junction vs. room temperature, in visual range we measured few relative percent increase while in 940 nm band range we measured 1.46x increase in sensitivity. Measured pixel source follower and transaction factor gains vs. temperature contributed to pixel output signal slope. Measured impact of sensitivity for visual bands, such as blue, green, and red colors, reflected some impact to captured image color accuracy that created slight image color tint at high temperature. The tint is, however, hard to detect visually and may be completely removed by auto white balancing and temperature adjusted color correction matrixes.

VI. Acknowledgement

The authors would like to thank Taner Ozcelik, Ross Jatou, and Rick Mauritzson for support and proofreading and Andrew Ko for valuable images.

References

[1] C. Silsby, S. Velichko, S. Johnson, Y. P. Lim, R. Mentzer, J. Beck, “A 1.2MP 1/3” CMOS Image Sensor with Light Flicker Mitigation”, in *Proc. IISW 2015*.

[2] S. Velichko, et al., “140dB Sub-electron Noise Floor Image Sensor”, in *Proc. IISW 2017*.

[3] M. Green and M. Keevers “Optical properties of intrinsic silicon at 300ºK”, *Progress in Photovoltaics*, vol.3, no.3; (1995), pp.189-192.

[4] M. Green, “Self-consistent optical parameters of intrinsic silicon at 300ºK including temperature coefficients”, *Solar Energy Materials & Solar Cells*, 92 (2008), pp. 1305– 1310.

[5] http://www.cie.co.at/

[6] S. Xie and A. Theuwissen “Compensation for Process and Temperature Dependency in a CMOS Image Sensor”, *Sensors*, 19, 870 (2019).